CHAPTER

S11

Indian Ocean: Supplementary Materials

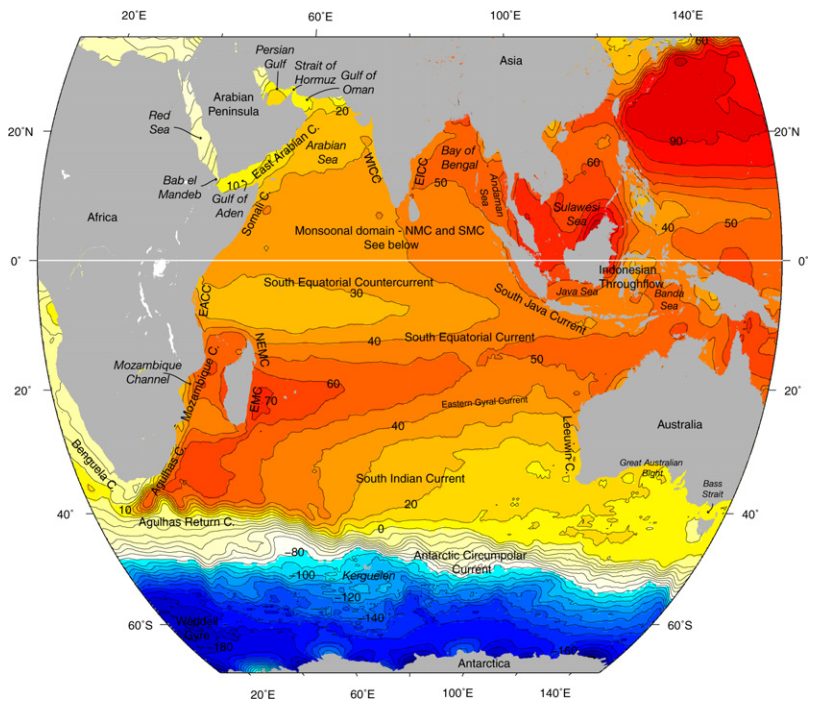

FIGURE S11.1 Indian Ocean surface circulation (Tables S11.1, S11.2 and Figure 11.1). Surface height (cm). Data from Niiler, Maximenko, and McWilliams (2003).

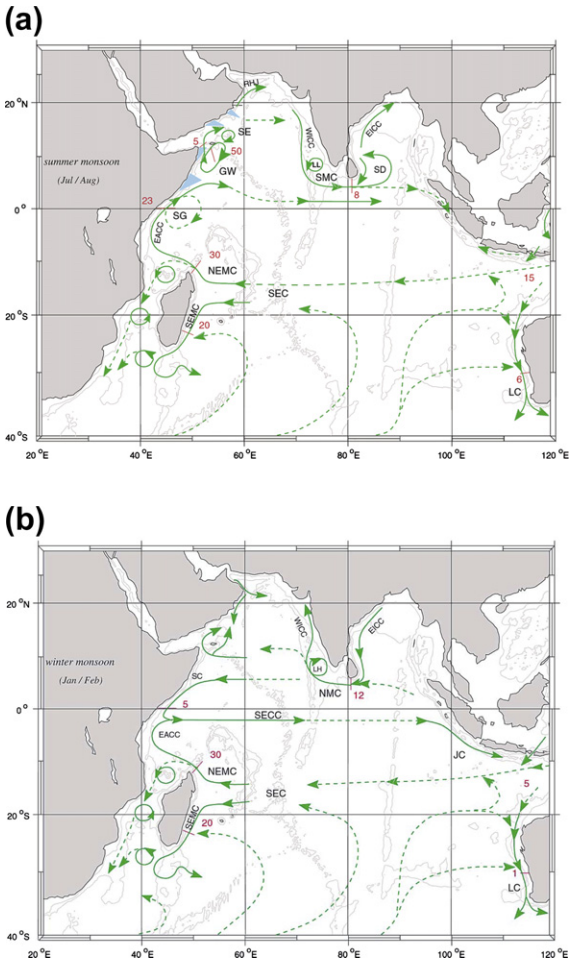

FIGURE S11.2 Surface circulation: (a) Southwest Monsoon (July–August) and (b) Northeast Monsoon (January–February). Most current names are in Table S11.2. Red numbers are transports (Sv) taken from Schott and McCreary (2001). *Source: Modified from Schott, Dengler, and Schoenefeldt (2002).*

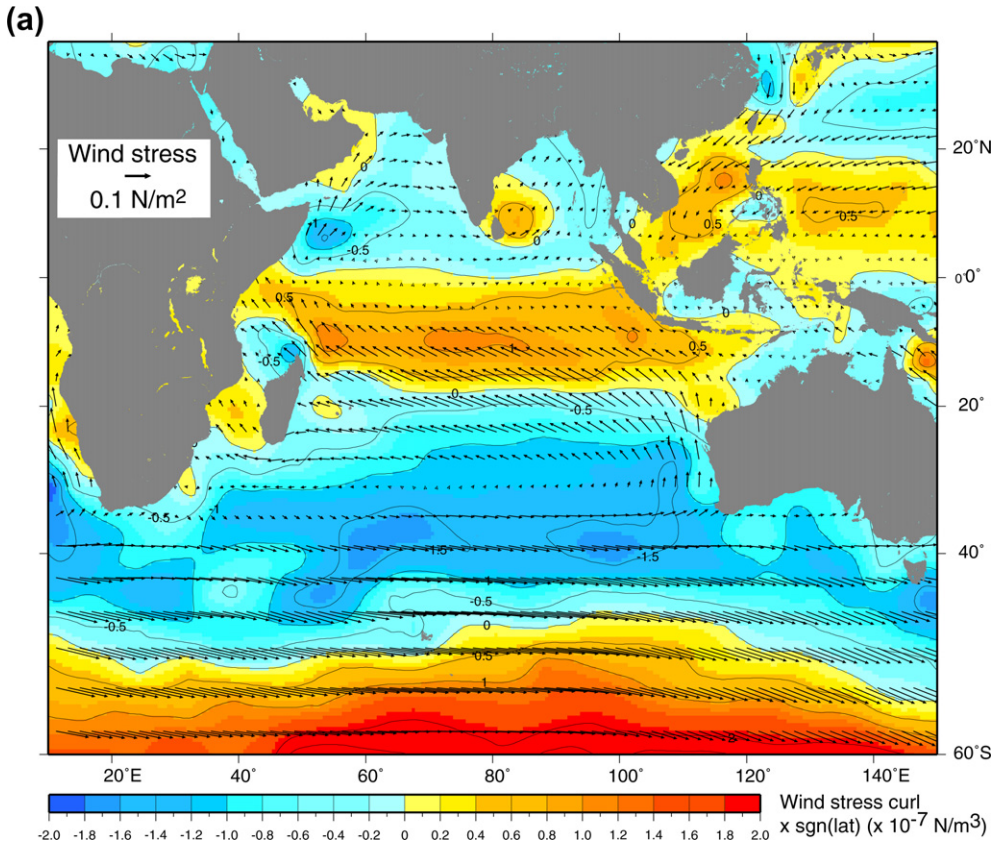

FIGURE S11.3 Annual mean winds. Data from the NCEP reanalysis (Kalnay et al.,1996). (a) Wind stress (N/m^2) (vectors) and wind-stress curl ($\times 10^{-7}$ N/m^3) (color), multiplied by -1 in the Southern Hemisphere. (b) Sverdrup transport (Sv), where blue is clockwise and yellow-red is counterclockwise circulation. See also Figures 5.16 and 5.17.

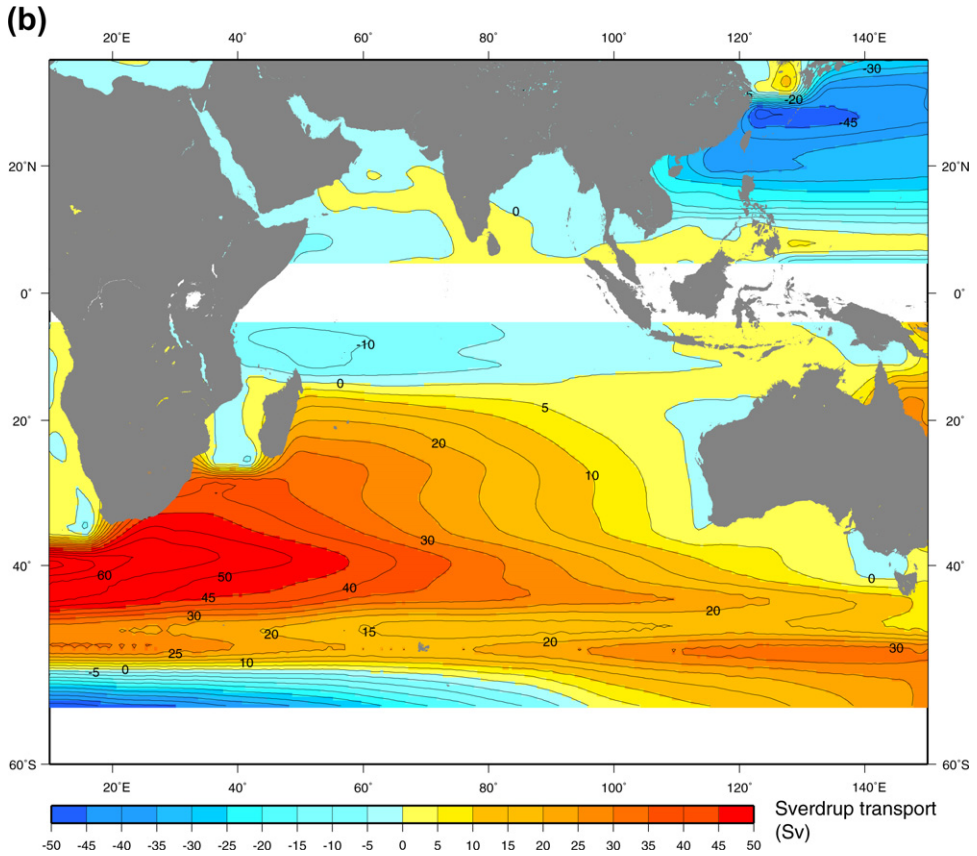

FIGURE S11.3 (*Continued*).

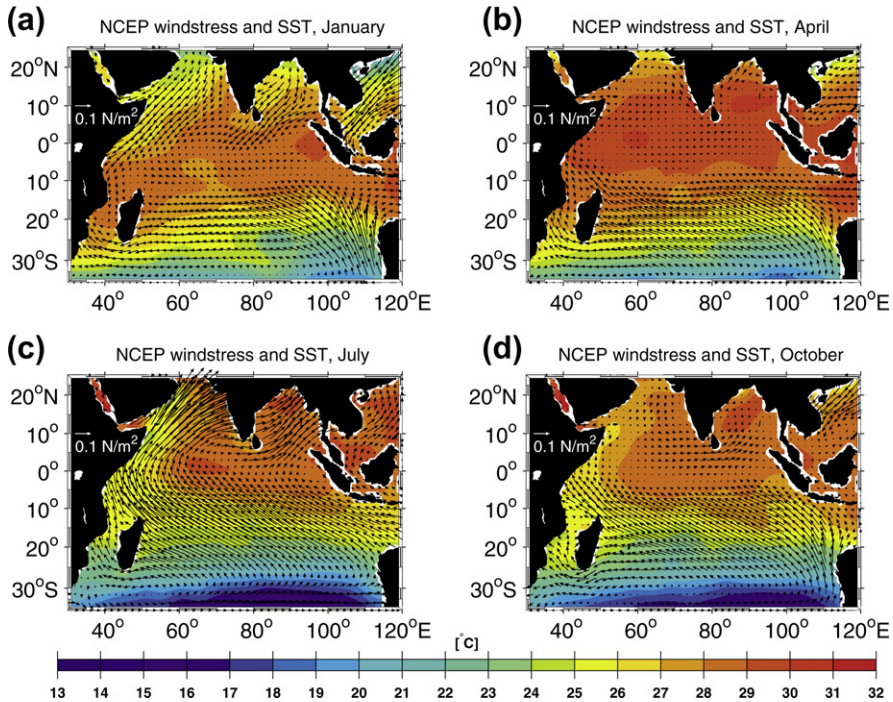

FIGURE S11.4 Monthly mean wind stress (N/m^2) from NCEP climatology. (a) January: Southwest Monsoon. (b) April: transitions. (c) July: Northeast Monsoon. (d) October: transitions. Monthly mean surface temperature (°C) from Levitus and Boyer (1994) is shown in color. *Source: From Schott, Dengler, and Schoenefeldt (2002).* See also Figure 5.16.

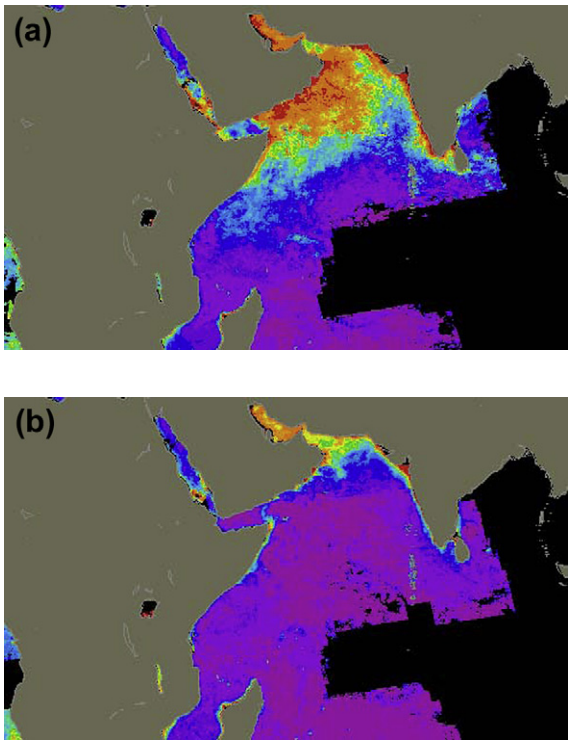

FIGURE S11.5 Ocean surface color for (a) July–Sept., 1979 (Southwest Monsoon) and (b) April–June, 1979 (Northeast Monsoon), indicating the presence of high productivity (high chlorophyll) by red, orange, and yellow colors. *Source: From NASA Goddard Earth Sciences (2008).*

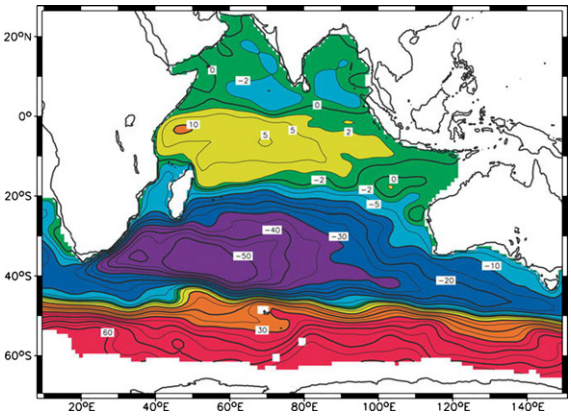

FIGURE S11.6 Geostrophic stream function (1000 m^2/s) at 900 m, from mean velocities measured by profiling floats. ©American Meteorological Society. Reprinted with permission. *Source: From Davis (2005).*

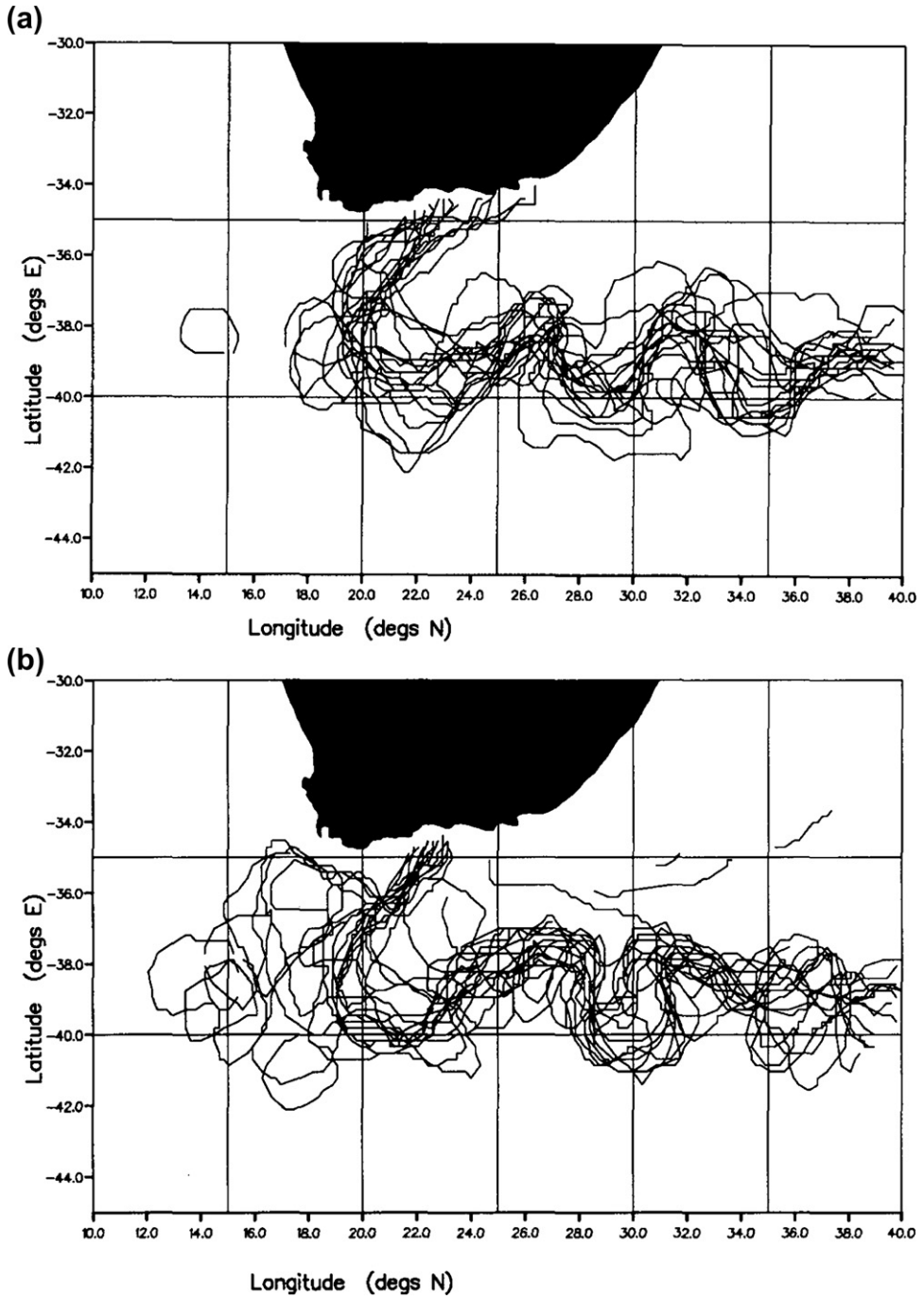

FIGURE S11.7 Infrared boundary of the Agulhas Current from 1985 to 1988: (a) December–February (summer) and (b) June–August (winter). ©American Meteorological Society. Reprinted with permission. *Source: From Quartly and Srokosz (1993).*

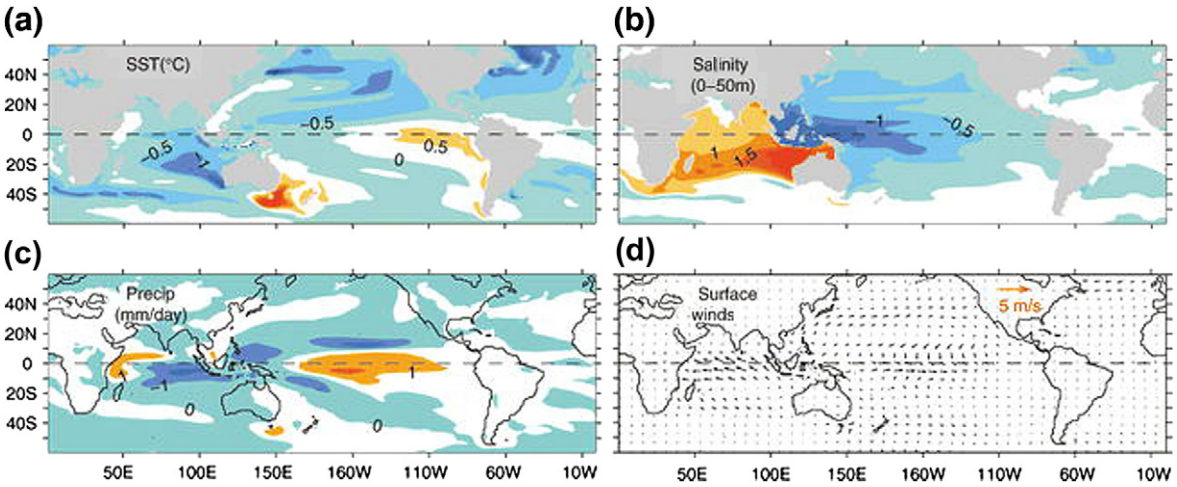

FIGURE S11.8 Changes in (a) surface temperature (°C), (b) surface salinity, (c) precipitation, and (d) surface winds due to the closure of the Indonesian throughflow in a coupled ocean-atmosphere model. ©American Meteorological Society. Reprinted with permission. *Source: From Song, Vecchi, & Rosati (2007).*

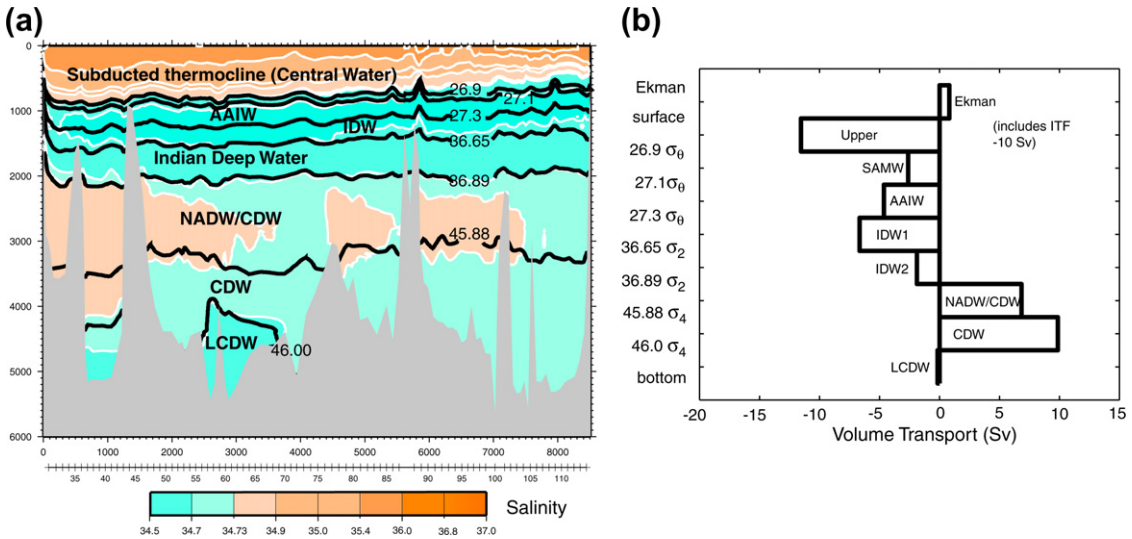

FIGURE S11.9 (a) Salinity at 32°S with isopycnal layers (black contours) and water mass labels (Table S11.3). (b) Meridional transport in the isopycnal layers. *Source: From Talley (2008).* See also Figure 11.15.

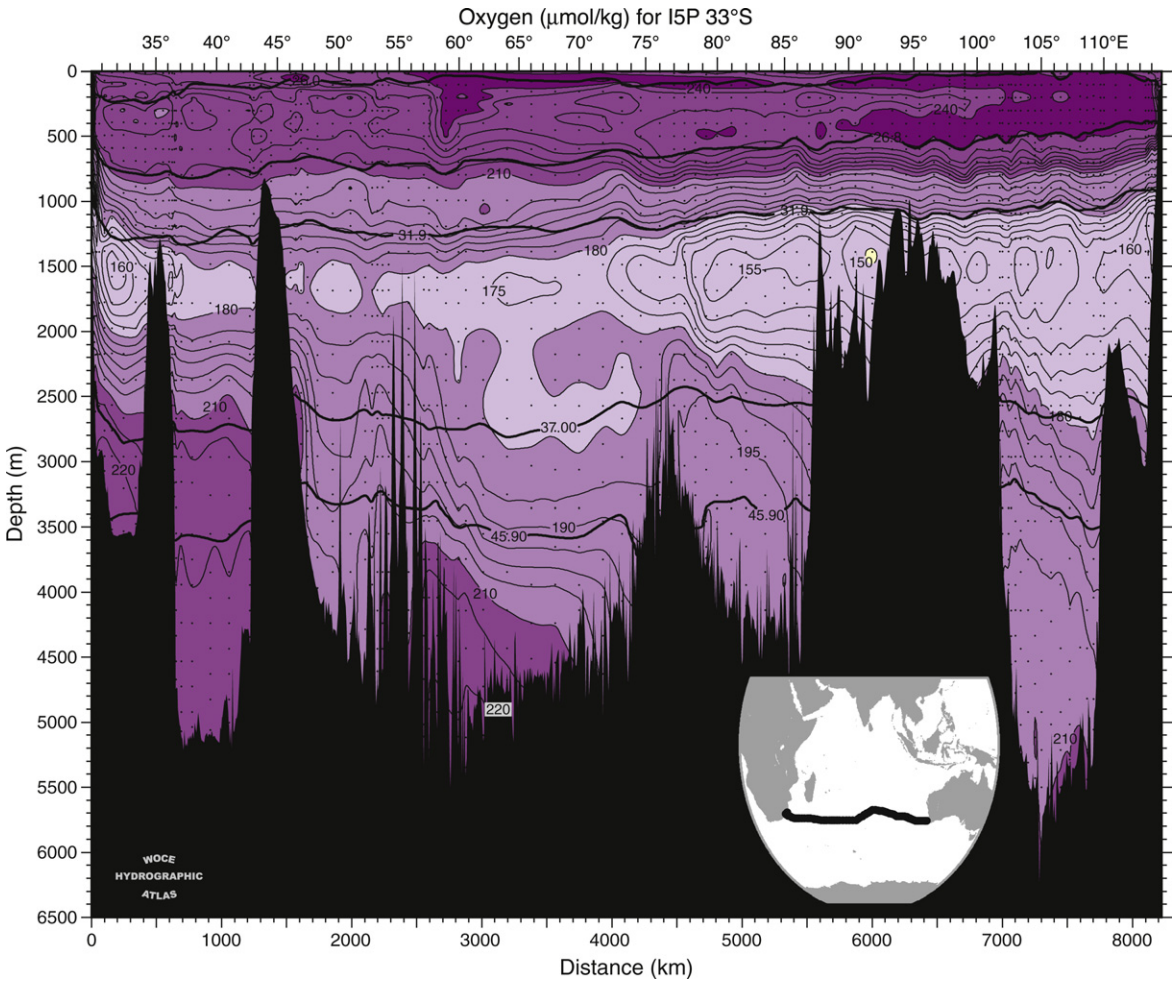

FIGURE S11.10 Oxygen (µmol/kg) at 33°S in 1987. Station locations are on the inset maps. *Source: From WOCE Indian Ocean Atlas, Talley (2011a); see also Toole and Warren (1993).* See also Figures 11.15, 11.16, and 11.21.

TABLE S11.1 Indian Ocean Mid-Latitude Circulation Elements (Southern Hemisphere)*

Name	Description
Subtropical gyre	Anticyclonic gyre at mid-latitudes
Agulhas Current	Western boundary current of the subtropical gyre along the coast of Africa
Agulhas Retroflection and Agulhas Return Current	Agulhas loop and return eastward flow off coast of southern Africa
Southeast Madagascar Current (SEMC)	Western boundary current of the subtropical gyre, flowing southward along the coast of Madagascar
South Indian Current (SIC)	Eastward flow of the subtropical gyre
Subantarctic Front (SAF)	Eastward flow in the northernmost front of the Antarctic Circumpolar Current
West Australia Current	Broad northward flow in the eastern subtropical gyre
Leeuwin Current	Poleward eastern boundary current along Australia
Leeuwin Undercurrent	Equatorward undercurrent beneath the Leeuwin Current
South Equatorial Current	Westward flow of the subtropical gyre
Deep Western Boundary Currents	Northward flow on the western side of the deep basins

* *Shading indicates the basic set.*

TABLE S11.2 Indian Ocean Tropical and Monsoonal Circulation Systems (Southwest Monsoon: July–August; Northeast Monsoon: January–February)

Name	Description
Arabian Sea circulation	Reversing with monsoon
Somali Current (SC)	Low latitude, monsoonally reversing western boundary current for the Arabian Sea circulation
Southern Gyre (SG)	Large eddy at western boundary on the equator during the Southwest Monsoon
Great Whirl (GW)	Large eddy at western boundary at 10°N during the Southwest Monsoon
West Indian Coastal Current (WICC)	Eastern boundary current of Arabian Sea gyre, along west coast of India, reverses with monsoon
Bay of Bengal circulation	Reversing with monsoon
East Indian Coastal Current (EICC)	Western boundary current in the Bay of Bengal, along east coast of India, reverses with monsoon
Northeast Monsoon Current (NMC), also called North Equatorial Current (NEC)	Westward flow north of and at the equator during the northeast monsoon
Southwest Monsoon Current (SMC)	Eastward flow north of and at the equator during the southwest monsoon
South Equatorial Countercurrent (SECC)	Eastward open ocean zonal flow south of equator
South Java Current (SJC)	Southward eastern boundary current connecting the SECC and SEC during the Northeast Monsoon
South Equatorial Current (SEC)	Westward open ocean zonal flow
Northeast Madagascar Current (NEMC) and East African Coastal Current (EACC)	Low-latitude western boundary currents along coast of Madagascar and coast of Africa, flowing northward connecting the SECC and SEC

TABLE S11.3 Principal Indian Ocean Water Masses*

Water Mass	Characteristic in the Vertical	Layer	Process
South Indian Central Water (CW)	Subtropical thermocline waters	Upper 0–1000 m	Subduction
South Indian Subtropical Underwater (STUW)	Subtropical/tropical salinity maximum	Upper 100–200 m	Subduction of high salinity subtropical surface waters
Subtropical Mode Water (STMW)	Subtropical stability (potential vorticity) minimum	Upper 0–300 m	Subduction of thick winter mixed layer from Agulhas Current
Subantarctic Mode Water (SAMW) and Southeast Indian SAMW (SEISAMW)	Subantarctic stability (potential vorticity) minimum	Upper 0–700 m	Subduction of thick winter mixed layer from Subantarctic Front
Arabian Sea surface water	Warm, high salinity surface water	Upper 0–200 m	Net evaporation in Arabian Sea, Persian Gulf, and Red Sea
Bay of Bengal surface water	Warm, low salinity surface water	Upper 0–100 m	Net runoff and precipitation in Bay of Bengal
Gulf Overflow Water (GOW)	High salinity subsurface water	Upper 200–350 m	Evaporation and cooling in Persian Gulf and overflow into Arabian Sea
Indonesian Throughflow Water (ITFW)	Low salinity in South Equatorial Current	Upper 0–500 m	Throughflow from Pacific Ocean
Indonesian Intermediate Water (IIW)	Low salinity in South Equatorial Current	Intermediate 800–1200 m	Throughflow from Pacific Ocean
Red Sea Overflow Water (RSOW)	Salinity maximum	Intermediate 400–1200 m	Evaporation and cooling in Red Sea and overflow into Arabian Sea
Antarctic Intermediate Water (AAIW)	Salinity minimum	Intermediate 500–1200 m	Advection of fresh subantarctic surface water
Indian Ocean Deep Water (IDW)	Oxygen minimum, nutrient maximum	Deep 2000–3500 m	Mixing and aging of deep waters including RSOW
North Atlantic Deep Water (NADW)	Salinity maximum	Deep 2200–3500 m	Atlantic Ocean
Upper Circumpolar Deep Water (UCDW)	High oxygen, low nutrients, high salinity on isopycnal surfaces	Deep ~1000–3000 m	Mixture of deep waters in the Southern Ocean
Lower Circumpolar Deep Water (LCDW)	Deep salinity and oxygen maxima, nutrient minima	Bottom 3000 m to bottom	Brine rejection in the Southern Ocean mixed with NADW, PDW and IDW

** Shading indicates the basic set.*

Reference

Davis, R.E., 2005. Intermediate-depth circulation of the Indian and South Pacific Oceans measured by autonomous floats. J. Phys. Oceanogr. 35, 683–707.

Kalnay, E., Kanamitsu, M., Kistler, R., Collins, W., Deaven, D., Gandin, L., et al., 1996. The NCEP-NCAR 40-year reanalysis project. Bull. Am. Meteorol. Soc. 77, 437–471.

Levitus, S., Boyer, T.P., 1994. World Ocean Atlas 1994 Volume 4: Temperature. NOAA Atlas NESDIS 4. U.S. Department of Commerce, Washington, D.C., 117 pp.

NASA Goddard Earth Sciences, 2008. Ocean color: classic CZCS scenes, Chapter 4. NASA Goddard Earth Sciences Data Information Services Center. http://disc.gsfc.nasa.gov/oceancolor/scifocus/classic_scenes/04_classics_arabian.shtml (accessed 1.9.09).

Niiler, P.P., Maximenko, N.A., McWilliams, J.C., 2003. Dynamically balanced absolute sea level of the global ocean derived from near-surface velocity observations. Geophys. Res. Lett. 30, 22. doi:10.1029/2003GL018628.

Quartly, G.D., Srokosz, M.A., 1993. Seasonal variations in the region of the Agulhas retroflection: studies with Geosat and FRAM. J. Phys. Oceanogr. 23, 2107–2124.

Schott, F.A., Dengler, M., Schoenefeldt, R., 2002. The shallow overturning circulation of the Indian Ocean. Progr. Oceanogr. 53, 57–103.

Schott, F.A., McCreary Jr., J., 2001. The monsoon circulation of the Indian Ocean. Progr. Oceanogr. 51, 1–123.

Song, Q., G.A., Vecchi, G.A., Rosati, A.J., 2007. The role of the Indonesian Throughflow in the Indo-Pacific climate variability in the GFDL coupled climate model. J. Clim. 20, 2434–2451.

Talley, L.D., 2008. Freshwater transport estimates and the global overturning circulation: shallow, deep and throughflow components. Progr. Oceanogr. 78, 257–303. doi:10.1016/j.pocean.2008.05.001.

Talley, L.D., 2011a. Hydrographic Atlas of the World Ocean Circulation Experiment (WOCE). Volume 3: Indian Ocean. Sparrow, M., Chapman, P., Gould, J. (Eds.), International WOCE Project Office, Southampton, U.K. Online version: http://www-pord.ucsd.edu/whp_atlas/indian_index.htm (accessed 4.20.09).

Toole, J.M., Warren, B.A., 1993. A hydrographic section across the subtropical South Indian Ocean. Deep-Sea Res. I 40, 1973–2019.